UNIVERSITY OF PARDUBICE

FACULTY OF CHEMICAL TECHNOLOGY

INSTITUTE OF CHEMISTRY AND TECHNOLOGY OF MACROMOLECULAR MATERIALS

Hamza Aboelanin

Synthesis and Characterization of Branched Polymers

Thesis of the Doctoral Dissertation (Annotation)

Pardubice 2023

Study program: **Chemistry and technology of martials (P2833)**

Study field: **Surface Engineering**

Author: **MSc. Hamza Mahmoud Ahmed Mahmoud Aboelanin**

Supervisor: **Prof. Ing. Štěpán Podzimek, CSc.**

Year of the defense: **2023**

References

ABOELANIN, Hamza Mahmoud, *Separation and characterization of synthetic and natural macromolecules*. Pardubice, 2023, 123 pages. Dissertation thesis (PhD.). University of Pardubice, Faculty of Chemical Technology, Institute of Chemistry and Technology of Macromolecular Materials. Supervisor Prof. Ing. Štěpán Podzimek, CSc.

Abstract

The dissertation deals with the separation and characterization of the molar mass and molar mass distribution and molecular structure in details of different types of branched polymers (methacrylate branched polymers and polyolefins). The molar mass and molar mass distributions, and branching studies for all the prepared methacrylate's branched polymers were determined by size exclusion chromatography with a multi-angle light scattering detector DAWN NEON, an RI detector Optilab NEON and an online viscometer ViscoStar NEON. While the separation and monitoring methyl (CH_3–) and methylene (–CH_2–) groups of series of ethylene/1-alkene and ethylene-propylene-diene copolymers (polyolefins) by high temperature-size exclusion chromatography with a filter-based infrared detector (IR5).

Keywords

Size exclusion chromatography, Multi-angle light scattering, Specific refractive index increment, Branched polymers, Polyolefins, Intrinsic viscosity, Branching ratio, chemical composition distribution, Filter-based infrared detector (IR5).

Table of Contents

Introduction

Branching can affect various chemical and physical properties of polymers, such as thermodynamic interactions between the polymer and the solvent [1–3], rheological properties [4,5], glass transition temperature [6], melting behavior and crystallization [7], phase separation of polymer blends [8,9], mechanical properties, solubility, chemical stability, and solution viscosity. In randomly branched polymers, the number of branching units in a polymer chain increases with increasing molar mass, and branching leads to a high molecular weight tail of the molar mass distribution [10].

The classical branching paper by Zimm and Stockmayer [11] offers the following equations relating the number of arms (f) with the branching ratio (g):

$$g = \frac{6f}{(f+1)(f+2)} \tag{1}$$

$$g = \frac{3f-2}{f^2} \tag{2}$$

Equation 1 was derived for star polymers where the arm length is polydisperse, i.e., the arms are not of equal length, whereas Equation 2 was derived for the stars with equal arm length. The branching ratio (contraction factor) is defined as the ratio of the mean square radii of branched (*br*) and linear (*lin*) molecules of the same molar mass (M):

$$g = \left(\frac{R_{br}^2}{R_{lin}^2}\right)_M \tag{3}$$

Where R is the root means square (RMS) radius (radius of gyration), and the subscript M indicates that the comparison is performed for the macromolecules of equal molar mass. A general limitation of the above equations is that they are valid for theta conditions, whereas the SEC measurements are typically performed in thermodynamically good solvents. As the thermodynamic quality of the solvent decreases with increasing degree of branching, the expansion of the branched macromolecules in thermodynamically good solvent is less than that of linear polymer chains. Consequently, the experimental values of g become smaller compared to the theta state.

Alternative branching ratio based on the intrinsic viscosity ($[\eta]$) was suggested by Zimm and Kilb [12]:

$$g' = \left(\frac{[\eta]_{br}}{[\eta]_{lin}}\right)_M \tag{4}$$

The two branching ratios are related by a simple equation:

$$g' = g^e \tag{5}$$

The main limitation is given by the fact that the relation of g' to the number of arms in star polymers or number of branch units in randomly branched macromolecules is less certain as it is via the parameter e which is related to the drainability of polymer chains. The draining parameter e is supposed to fall in the range of 0.5–1.5, yet the exact value is mostly unknown. The detailed discussion of hydrodynamic properties of branched polymers can be found in papers by Kurata et. al. [13,14] and Lederer et. al. [15].

Literature offers several equations relating the number of arms directly with the intrinsic viscosity-based branching ratio [12,16,17]:

$$g' = \frac{(2/f)^{1.5}[0.396(f-1)+0.196]}{0.586} \quad (6)$$

$$g' = \left(\frac{3f-2}{f^2}\right)^{0.58} \frac{0.724-0.015(f-1)}{0.724} \quad (7)$$

$$log\ g' = 0.36 - 0.8\ log\ f \quad (8)$$

The importance of short chain branching (SCB) in the properties of polymers is well-known. Stiffness, ductility, tear strength, clarity, and softening temperature are among the many performance characteristics affected profoundly by structure, frequency, and distribution SCB [18, 19]. Sun et al. [20] the short branch effect in α-olefin copolymers on root mean square (RMS) radius and intrinsic viscosity [η] in trichlorobenzene at 135 °C. This study of the effect of SCB on series of homopolymers of methacrylate and their copolymers with different alkyl groups was inspired by Sun et al. [20].

Studying the molar mass distribution (MMD), long-chain branching, and short-chain branching distribution of polyolefins is very important to understand their chemical and physical properties during processing and applications. The catalyst type used in the preparation of polyolefins has an important effect on the final properties of polymers. Metallocene and Ziegler–Natta catalysts have been widely employed for the in-situ polymerization of polyolefins [21]. Polyolefins produced by Metallocene catalysts, also called single-site catalysts, systems have long been claimed to produce polymers with narrow MMD or copolymers with uniform comonomer distribution [22,23] while Polyolefins made with Ziegler–Natta catalysts have non-uniform distributions of molar mass and chemical composition distribution.[24].

Hyphenation of infrared detection to size exclusion chromatography (SEC) expands possibilities of SEC even more and allows to reveal comonomer incorporation across molecular weight and thus help in the study of catalytic systems used in polyolefin synthesis. Coupling HT SEC with filter-based infra-red (IR) detector gives an easy and fast access to so-called short chain-branching (SCB) distribution vs MMD.

Experimental

Materials

n-butyl methacrylate (BMA), Methyl methacrylate (MMA), Benzyl methacrylate (BZMA), Ethylene Glycol Dimethacrylate (EGDMA), Lauryl methacrylate (LMA) and 2-ethyl hexyl methacrylate (2-EHMA) were purchased from Sigma-Aldrich, United States. Tetrahydrofuran (THF) (99.8%) and *n*-hexane were purchased from VWR Chemicals, United States. Methyl trimethylsilyl dimethyl ketene acetal (Me initiator), azobisisobutyronitrile (AIBN) and tetrabutylammonium acetate (*t*BuAAc) were purchased from Sigma-Aldrich.

The polyolefin samples were obtained from Fraunhofer partners working in universities, research institutes or industry.

Synthesis of star-like polymer

The star-like polymer samples were prepared by group transfer polymerization using the arm-first method in 250 mL round-bottom flasks, fitted with rubber septa. The solvent (THF), initiator and catalyst (*t*-BuAAc) were first transferred to the flask then the monomers were dosed slowly forming arm. After finishing the addition of monomer, arm solution let stirring for 20 min. then a 10 mL of arm solution was removed for further characterization. After that, the synthesis was completed by the addition of EGDMA cross-linker. Finally, the polymerization was terminated by adding commercial methanol (see scheme 1). The molar ratios of particular reagents for all prepared star-like samples are listed in Table 1.

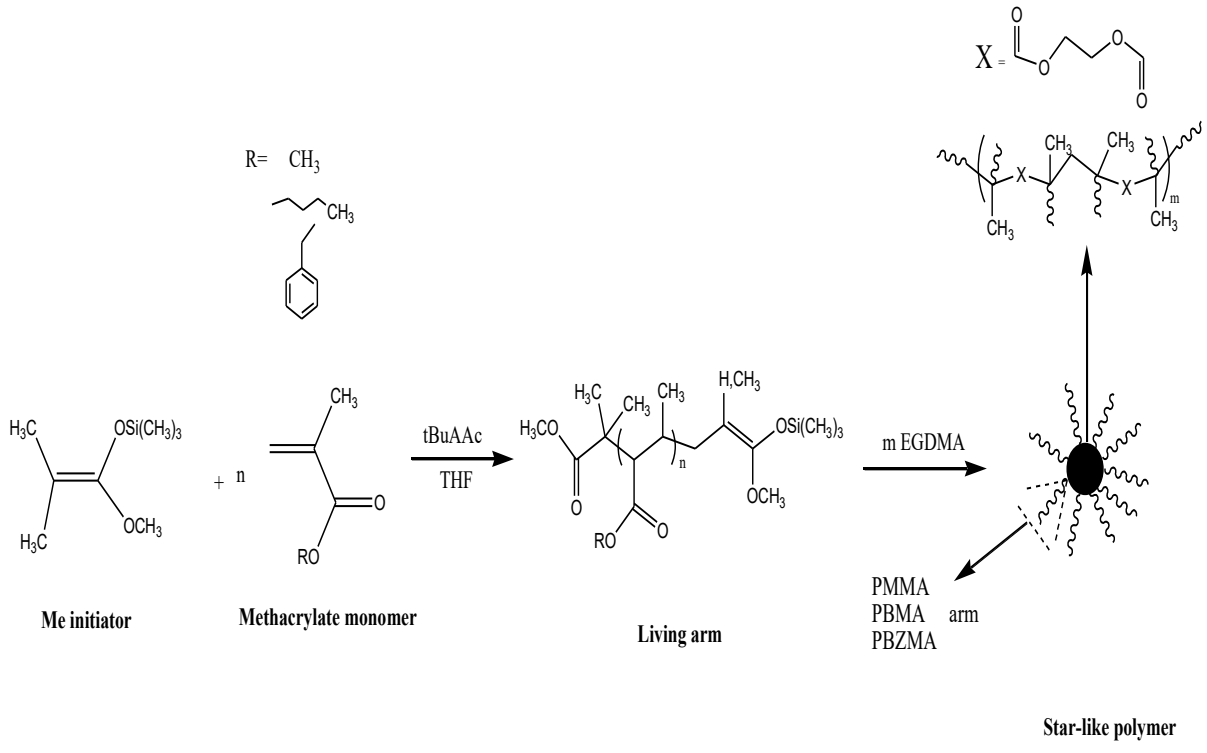

Scheme 1 Synthesis procedures of methacrylate star-like polymers.

Table 1 Molar ratios of reagents used for star-like polymer synthesis.

Sample	Monomer	Molar ratio		
		Initiator	Monomer	EGDMA
B2	BMA	1	49	3.7
B10	BMA	4	49	9.3
M1	MMA	1	30	1.3
M10	MMA	2.5	30	4.0

Synthesis of linear homo and co polymethacrylates

Linear homo- and co-polymethacrylates were prepared by solution free radical polymerization using azobisisobutyronitrile (AIBN) as initiator. About 50 mL of 50% solution of monomer in toluene was placed into a 100 mL closed vial and heated at 80 °C for 8 hr (Table 2). Scheme 2 represented preparation steps of Linear methacrylate polymers.

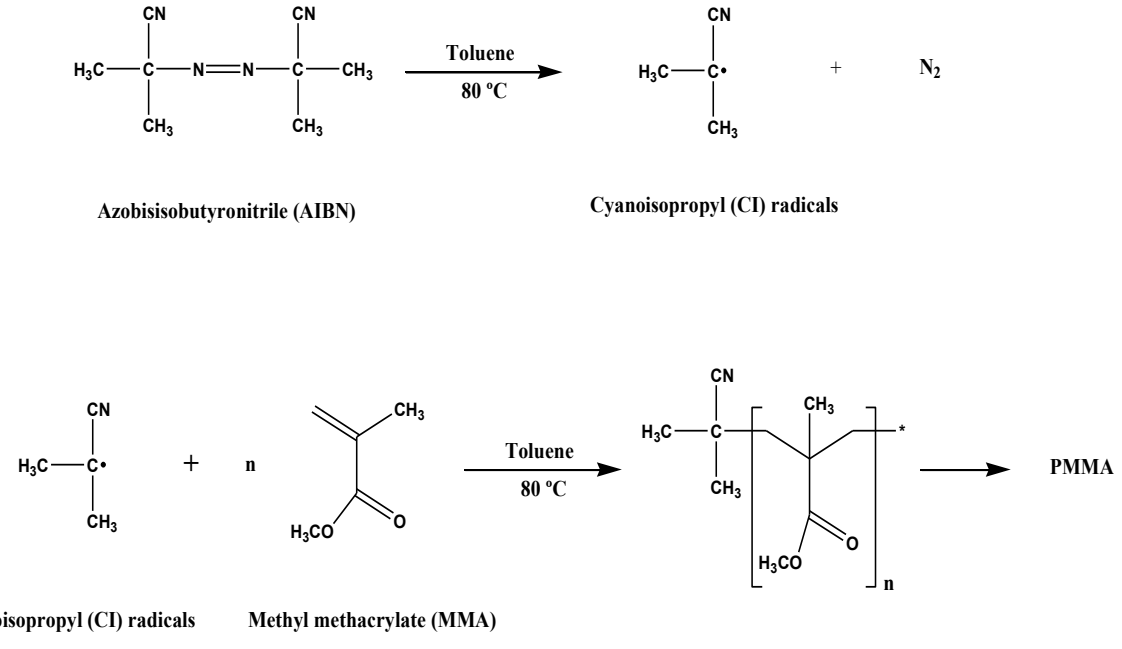

Scheme 2 Preparation of PMMA by free radical polymerization in Toluene.

Table 2 Synthesis of linear homo polymethacrylate samples.

Sample	Monomer	Initiator (wt%)	Monomer (mol%)	Solid (%)
PMMA	LMA	0.1	100	40
PBMA	BMA	0.1	100	32
PLMA	LMA	0.5	100	44

Polyolefin samples

A part of these samples has been described before (see references in Tables 3,4). Where average molar masses and/or dispersity were not known from previous investigations, they were evaluated based on current HT-SEC-IR5 measurements and are given as polyethylene-equivalent molar masses.

Table 3 Characteristics of ethylene-propene copolymers synthesized with metallocene catalyst.

Content of ethylene [mol %]	M_w [kg/mol]	$Đ$	Reference
1.5	166.9	3.8	[25]
6.34	150.2	3.4	
7.9	105	4.7	
8.5	124.4	3.9	
13.2	92.9	4.0	
36.0	63.2	4.2	
97.84	370.1	7.0	

Table 4 Characteristics of ethylene-1-hexene copolymers.

Content of 1-hexene [mol %]	M_w [kg/mol]	$Đ$	Reference
1.0	160	2.0	[26]
1.2	56	2.0	
1.4	278	2.0	
2.8	58	2.2	
7.0	52	2.1	
8.4	223	2.2	
12.8	24	2.0	

Instrumentation for SEC-MALS-Visco

The molar mass distributions, the conformation plots (RMS radius versus molar mass), and the Mark-Houwink plots were determined by SEC with a multi-angle light scattering (MALS) detector DAWN NEON, an RI detector Optilab NEON and an online viscometer ViscoStar NEON (all detectors from Wyatt Technology). The SEC system consisted of a 1200 Series isocratic pump and autosampler with two Mixed-C 300 × 7.5 mm 5 µm columns (all Agilent Technologies) using THF as the mobile phase at a flow rate of 1 mL/min. Samples were prepared at concentrations of ≈2.5 mg/mL (stars and linear homopolymers), ≈5 mg/mL (long arms), and ≈10 mg/mL (short arms). The samples were filtered with 0.45 µm syringe filters and injected in the amount of 100 µL. The data collection and processing were performed by Wyatt Technology software ASTRA. In addition to the calculations and plots provided by ASTRA, the data were exported from ASTRA as csv files for additional processing in Excel.

High-temperature size exclusion chromatography with a filter-based multiple band IR detector (HT SEC-IR5)

HT SEC-IR5 measurements were performed using a PolymerChar GPC-IR® (PolymerChar, Valencia, Spain), equipped with a 200 µL sample loop, at 150 °C. The mobile phase was 1,2,4-trichlorobenzene (TCB) (Across Organics, Schwerte, Germany) containing 0.5 g/L butylhydroxytoluene (BHT, Merck, Darmstadt, Germany). The mobile phase flow rate was 1 mL/min. Three POLEFIN linear XL analytical columns, 300 x 8.0 mm (Polymer Standards Service, Mainz, Germany) were used for the analysis. Detection was performed with a filter-based multiple band IR detector (model IR5-MTC, PolymerChar, Valencia, Spain) featuring a thermoelectrically cooled mercury-cadmium-telluride (MCT) sensor. The IR5 detector includes two narrow band filters tuned to the adsorption region assigned to–CH_3 (at 2960 cm^{-1}) and –CH_2–

(2920 cm^{-1}) groups, as well as a broader filter used to collect absorbance from all C-H bonds in a polymer [27−29]. The heated flow-through cell volume and the path-length are 13 µL and 1.8 mm, respectively. The cell is equipped with sapphire windows.

The MMD was evaluated using a polystyrene (PS) calibration (EasiCal PS-1, Agilent, Waldbronn, Germany) and WinGPC software version 8 (Polymer Standards Service GmbH, Mainz, Germany). The molar masses of PS standards were transferred to polyethylene (PE) equivalents using the following Mark-Houwink coefficients from the literature: K: 3.8 x 10^{-2} mL/g, α: 0.73 for polyethylene and K: 1.26 x 10^{-2} mL/g, α: 0.702 for poly styrene [29].

For each measurement, approx. 12 mg polymer were automatically mixed with 6 mL mobile phase. Simultaneously, the vials were flushed with nitrogen. Each sample was dissolved under shaking in the autosampler for 1 h at 150 °C before injection.

Results and discussion

Molar mass and molar mass distribution determination of star-like and linear polymers

Figure 1 depicts a typical molar mass versus elution volume plot of some selected PBMA and Linear homo methacrylate polymers.

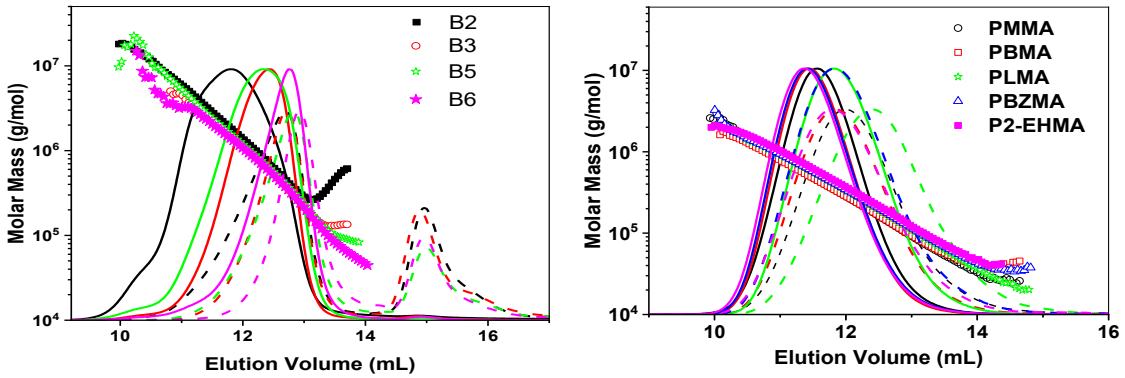

Figure 1 Molar mass versus elution volume plots of star-like PBMA with long arms (left) and linear homo methacrylate polymers (right). MALS @ 90° (—, solid) and RI (---, dashed) chromatograms are overlaid.

The number-average (M_n) and the weight-average (M_w) molar masses, the values of dispersity ($Đ$), and the weight-average intrinsic viscosities ($[\eta]_w$) of arms and stars, and the star fractions in the final polymerization products for some selected prepared star-like polymers are listed in Table 5. And the same values for some selected linear methacrylate polymers are listed in Table 6.

Table 5 The values of M_n, M_w, $Đ$, $[\eta]_w$, and star fraction for some selected star-like polymer.

sample	M_n (kg mol^{-1})		M_w (kg mol^{-1})		$Đ$		$[\eta]$ (mL/g)		Star fraction (%)
	arm	star	arm	star	arm	star	arm	star	
B2	8.9	550	9.3	1132	1.05	2.06	6.1	13.6	74
B10	2.44	237	2.7	1712	1.11	7.22	3.8	12.8	87
M1	6.5	66	6.9	102	1.07	1.54	6.1	11.2	77
M10	1.9	84	2.1	388	1.07	4.62	3.8	8.90	87

Table 6 The values of M_n, M_w, $Đ$, $[\eta]_w$ for some selected linear methacrylate polymers.

Polymer	M_n (Kg mol^{-1})	M_w (Kg mol^{-1})	M_w/M_n	$[\eta]_w$ (mL/g)
PMMA	164	310	1.92	70.9
PBMA	215	497	1.68	80.8
PLMA	124	260	2.10	43.1

Solution properties of star-like polymers

The conformation plot is the most direct way to branching information. However, it has two limitations. It cannot be applied to polymers composed of the majority of molecules with RMS radii below ≈ 7 nm. Moreover, for many branched polymers it is strongly affected by the delayed elution of branched macromolecules as described for example in Reference [17]. Mark-Houwink plots of several star-like PMMAs composed of different arm length are compared in Figure 2. The slope (Mark-Houwink exponent) of the plots of star-branched polymers consisting of long arms is close to zero at the region of lower molar masses, which indicates sphere-like structure. Towards the high molar masses, the slope increases to the value of ≈ 0.28. The slope of the plots of samples consisting of short arms starts at ≈ 0.1 and increases to the same value as that of the stars from long arms. At lower molar masses, the plots of stars created by short arms are shifted to lower intrinsic viscosities which can be explained by higher number of arms at the same molar mass and thus more compact molecular structure. The difference diminishes towards high molar masses. The increase of the Mark-Houwink exponent towards high molar mass suggests the transition of the molecules from sphere-like structures to more expanded structures. One can imagine that the molecules of high molar mass consist of several compact EGDMA cores which are connected by less compact links.

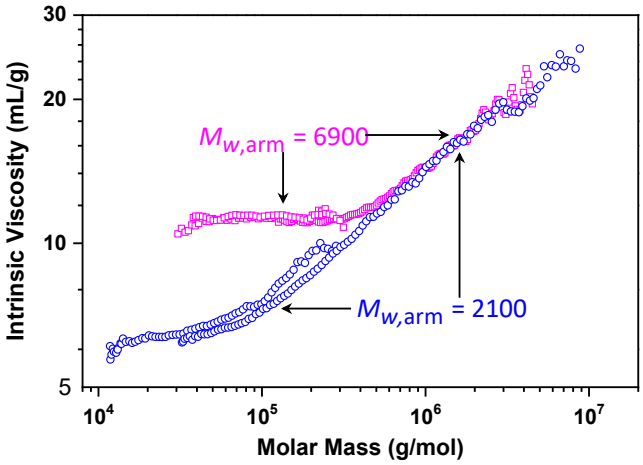

Figure 2 Mark-Houwink plots of star-like PMMAs with arm M_w ≈ 2100 g/mol (○, blue) and ≈ 6900 g/mol (□, magenta).

The obtained data allow testing various *g*–versus–*f* equations since the true number of arms at each molar mass can be calculated from the slice molar mass and molar mass of the arm prepared in the first reaction step. Instead of explicitly expressing the *f* as a function of *g* or *g´*, Equations 1, 3, 6–8 were entered into Excel, and *g* or *g´* were calculated for the stepwise increasing *f*, and then the experimental values of *g* or *g´* were matched in regular intervals with *f*. Figure 3 depicts various plots of the number of arms per molecule against molar mass for star-like PMMA sample for which the determination of the RMS radius was possible and which did not show a significant tendency to the delayed elution and such allowed testing also the Equations 1 and 3. The conclusion from Figure 3 is that none of the equations allow accurate determination of the number of arms from the ratios *g* or *g´*. However, a very good agreement between the plot obtained using Equation 6 and that calculated from the slice molar mass was obtained for stars created by short arms as shown

in Figure 4. The modification of Equation 6 in the sense of using exponent 1.6 instead of 1.5 gives good agreement for the stars consisting of long arms as shown in Figure 5. Similar results are obtained for star-like PBMA, i.e., Equation 6 markedly overestimates the number of arms per molecule in the case of long arms, whereas markedly better agreement is obtained for polymer consisting of short arms as shown in Figure 6. The polymer consisting of long arms requires increasing the exponent to the value of ≈ 1.7 as demonstrated in Figure 7. Comparison of samples M2 (arm M_w ≈ 6900 g/mol) and B2 (arm M_w ≈ 9300 g/mol) indicates that longer arms require higher exponent.

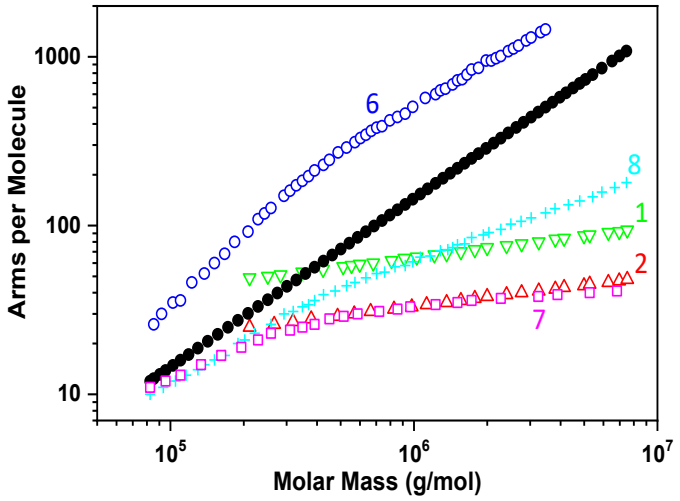

Figure 3 Plots of number of arms per molecules versus molar mass calculated by the division of slice molar mass by M_w of arms (●) and estimated from Equations 1, 2, 6, 7, and 8 for star-like PMMA with arm M_w ≈ 6900 g/mol (sample M2).

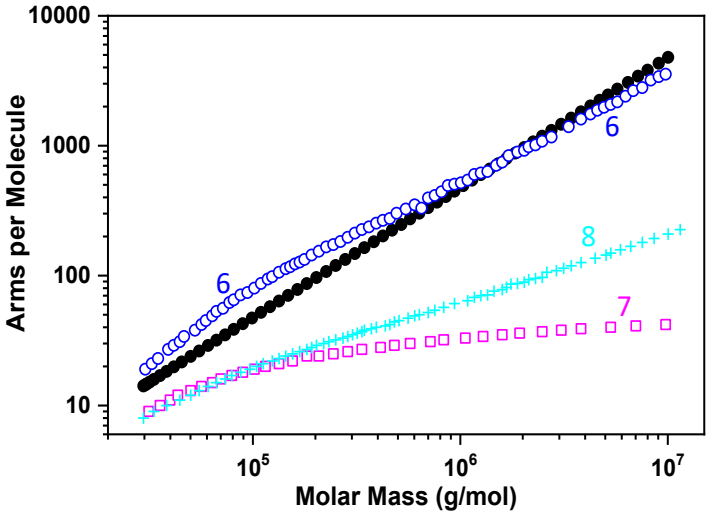

Figure 4 Plots of number of arms per molecule versus molar mass calculated by the division of slice molar mass by M_w of arms (●) and estimated from Equations 6, 7, and 8 for star-like PMMA with arm M_w ≈ 2100 g/mol (sample M10).

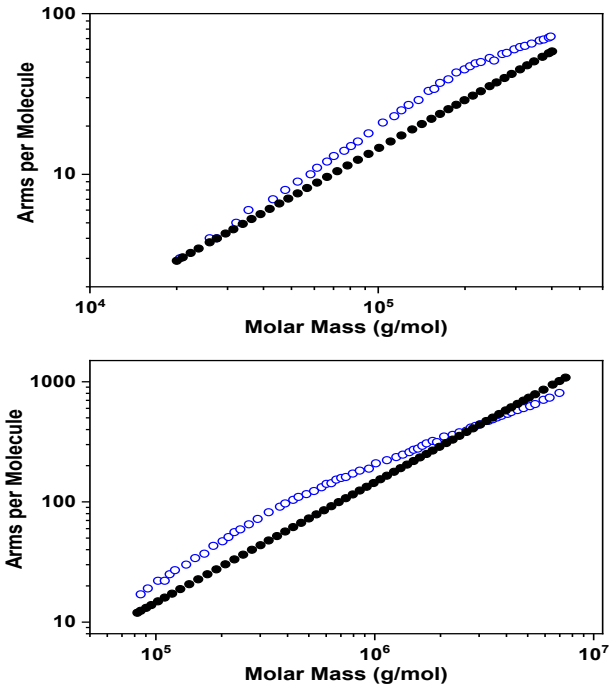

Figure 5 Plots of number of arms per molecule versus molar mass for two star-like PMMAs consisting of arms having $M_w \approx 6900$ g/mol calculated by the division of slice molar mass by M_w of arms (●) and estimated from Equation 6 using the exponent 1.6 instead of 1.5 (○, magenta; samples M1 top and M2 bottom).

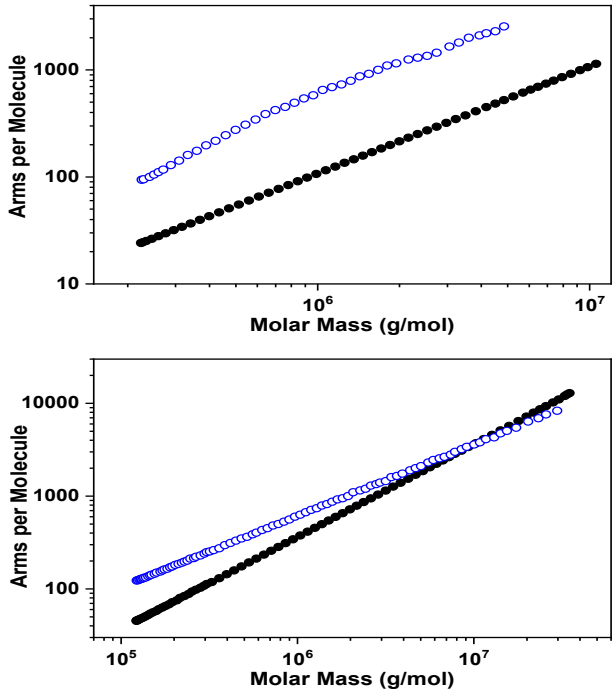

Figure 6 Number of arms per molecule versus molar calculated by the division of slice molar mass by M_w of arms (●) and estimated using Equation 6 for star-like PBMA with arm $M_w \approx$ 9300 g/mol (top, sample B2) and $M_w \approx 2700$ g/mol (bottom, sample B10).

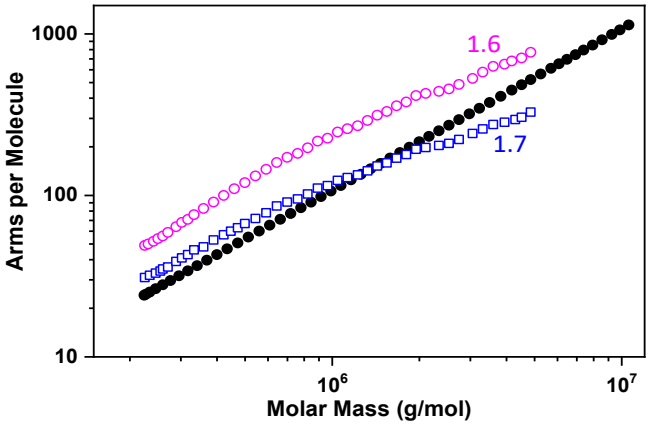

Figure 7 Plots of number of arms per molecule versus molar mass for star-like PBMA consisting of arms having $M_w \approx 9300$ g/mol calculated by the division of slice molar mass by M_w of arms (●) and estimated from Equation 6 using the exponent 1.6 (○, magenta) and 1.7 (□, blue), (sample B2).

The molar mass distribution exported from ASTRA to Excel can be converted to the distribution of arms per molecule by dividing the molar mass axis by the molar mass of arm. The plots obtained for various PMMA and PBMA star-like polymers are shown in Figure 8.

Exporting the slice molar masses and the slice concentrations permits the calculation of the number-average (f_n) and the weight-average (f_w) arms per molecule using the equations equivalent to those for the calculation of molar mass moments:

$$f_n = \frac{1}{\sum \frac{w_i}{f_i}} \tag{11}$$

$$f_w = \sum w_i f_i \tag{12}$$

where f_i is the number of arms in molecules eluting at the *i-th* elution volume V_i and w_i is the weight fraction of molecules eluting at that V_i calculated as the slice concentration c_i divided by the sum $\sum c_i$.

The results for samples shown in Figure 8 are listed in Table 7. Table 7 is further completed by the values of $g'(M_w)$. The average branching ratio $g'(M_w)$ is the ratio of the experimental weight-average intrinsic viscosity of the branched polymer divided by the intrinsic viscosity of a hypothetical linear polymer that would have the same M_w as the polymer requiring analysis. This ratio can be used for mutual comparison of different samples for which the molar mass of arms is unknown.

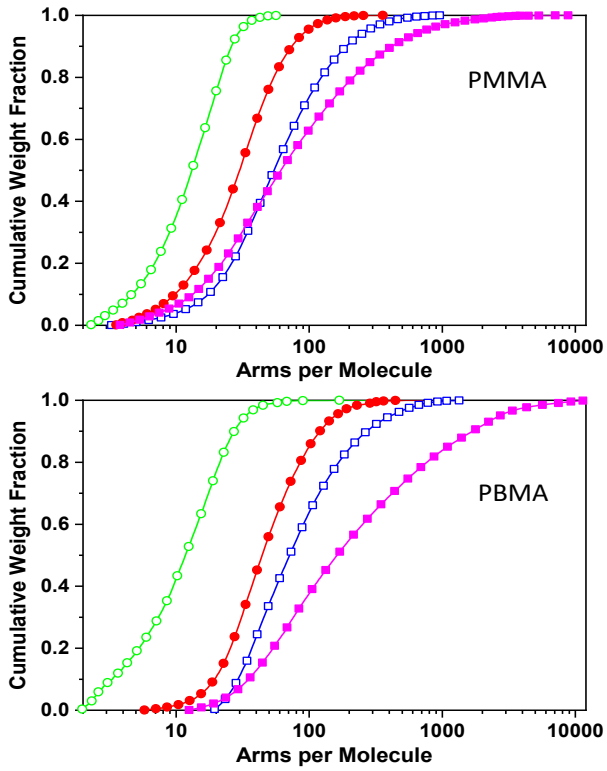

Figure 8 Cumulative distribution of arms per molecule for PMMA star-like polymers with long (samples M1○, green; M2 □,blue and M3 ●, red) and short (sample M10 ■, magenta) arms; and for PBMA star-like polymers with long (samples B2 □, blue; B3 ●, red and B4 ○, green) and short (sample B10 ■, magenta) arms.

Table 7 Number-average and weight-average arms per molecule and g′(M_w) for samples shown in Figure 9.

Sample	f_n	f_w	$g'(M_w)$
M1	9	24	0.326
M2	35	80	0.103
M3	19	35	0.173
M10	35	163	0.101
B2	52	110	0.069
B3	33	56	0.105
B4	8	13	0.300
B10	77	582	0.048

Short chain branching of linear methacrylate polymers

The RMS radius conformation plots (i.e., log-log relation RMS radius–molar mass) and Mark-Houwink plots (log-log relation intrinsic viscosity–molar mass) measured by SEC-MALS-Visco give valuable information about the molecular structure and dilute solution properties of the prepared linear homopolymers and PMMA with different comonomers. All conformation plots and Mark-Houwink plots for homopolymers are shown in Figure 9.

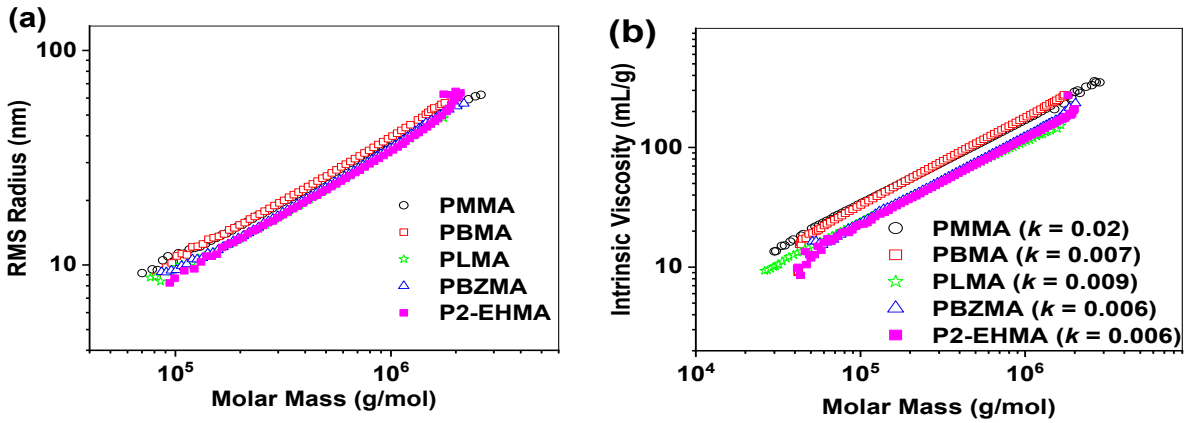

Figure 9 (a) conformation plots (with slope ~ 0.6 for all plots), (b) Mark-Houwink plots (with slope ~ 0.5 for all plots) of linear methacrylate polymers.

The slope of the conformation plots and the Mark-Houwink plots represented in Figure 9 of the linear methacrylate homopolymers are approximately the same (b ~ 0.6 slope of conformation plots and a ~ 0.7 slope of Mark-Houwink plots) indicating that the power law exponents of each relation are insensitive to the comonomer content. Also, the intercept of the Mark-Houwink plot of PMMA and PBMA homopolymers are very close, and the intercept of PBZMA, P2-EHMA and LMA homopolymers are approximately identical. The intercept is slightly shifted only when the side chains increase from C4 to C12, or when they are aromatic rings as evident from comparing PMMA and PBMA with LMA and PBZMA.

Chemical composition distribution of ethylene-alkene copolymers

The CH_3/CH_2 ratio reflects changes in the chemical composition of EP copolymer with the elution volume (Table 3) synthesized also with a metallocene catalyst as shown in Figure 10. While the EP sample containing 58.3 mol% ethylene shows a substantial decrease in the CH_3/CH_2 ratio with increasing molar mass, the EP sample with 13.2 mol% shows an increasing CH_3/CH_2 ratio (Figure 10). According to the calibration for these copolymer samples (Figure 11), the content of ethylene in the sample with 58.3 mol % decreased from 73 mol % to 52 mol %, while in the sample with 13.2 mol% it increased from 13 mol % to 16 mol% ethylene.

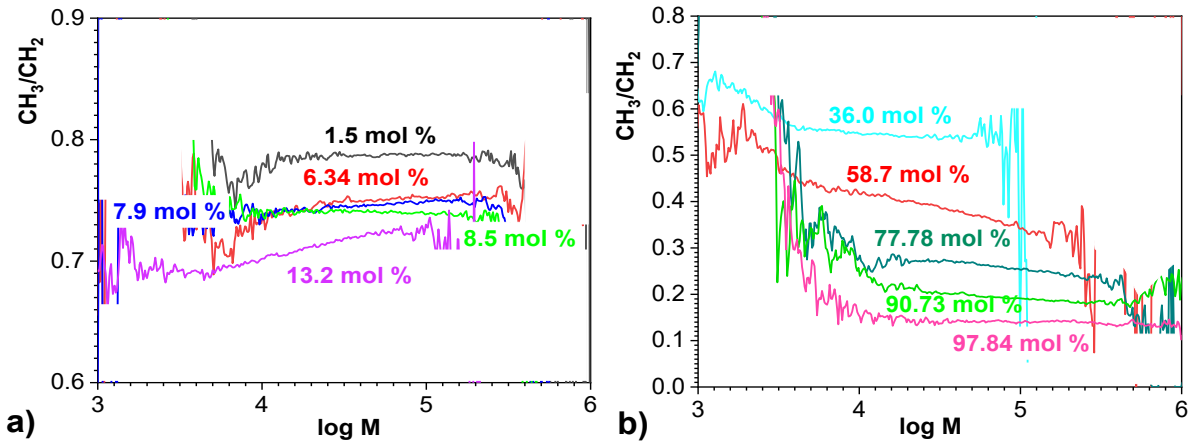

Figure 10 CH_3/CH_2 ratio as a function of equivalent PE molar mass of EP copolymers (Table 3).

Figure 12 is an example of considerable diversity in the CH_3/CH_2 profiles of EH copolymers (Table 4). While samples in the range of 1–4 mol % 1-hexene exhibit flat profiles, the CH_3/CH_2 ratio of samples containing 6.2 and 8.4 mol % 1-hexene increases and the CH_3/CH_2 ratio of samples containing 5.8, 7.0 and 12.8 mol % 1-hexene decreases. The sample containing 12.8 mol % is the most inhomogeneous (composition between 8 and 15 mol % 1-hexene). The chemical inhomogeneity of the samples is apparently the reason for the substantial scattering of data points around the calibration line in Figure 12b. This substantially decreases the quality of the calibration curves in comparison to previously reported ones (e.g., Frijns-Bruls et al. [30]). Considering the calibration line, the ethylene content in the sample containing 12.8 mol % ethylene decreases from 20 mol % to 9 mol % with increasing molar mass, while in the sample containing 6.2 mol % ethylene it increases from 7 mol % to 17 mol %. These are substantial changes in the 1-hexene content along the molar mass axis.

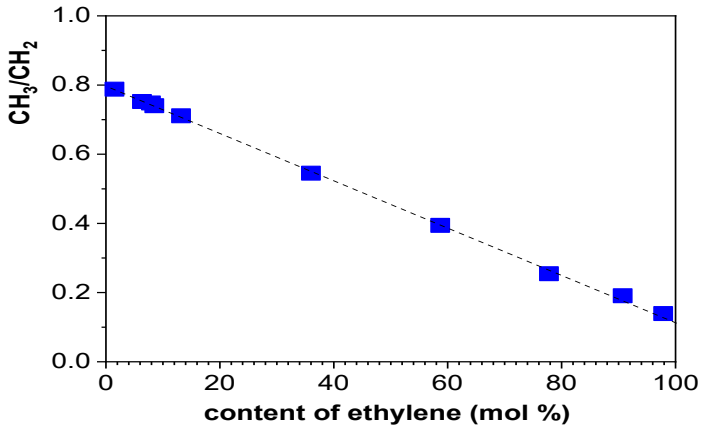

Figure 11 CH_3/CH_2 ratio as function of the average content of ethylene in EP copolymers (Table 3).

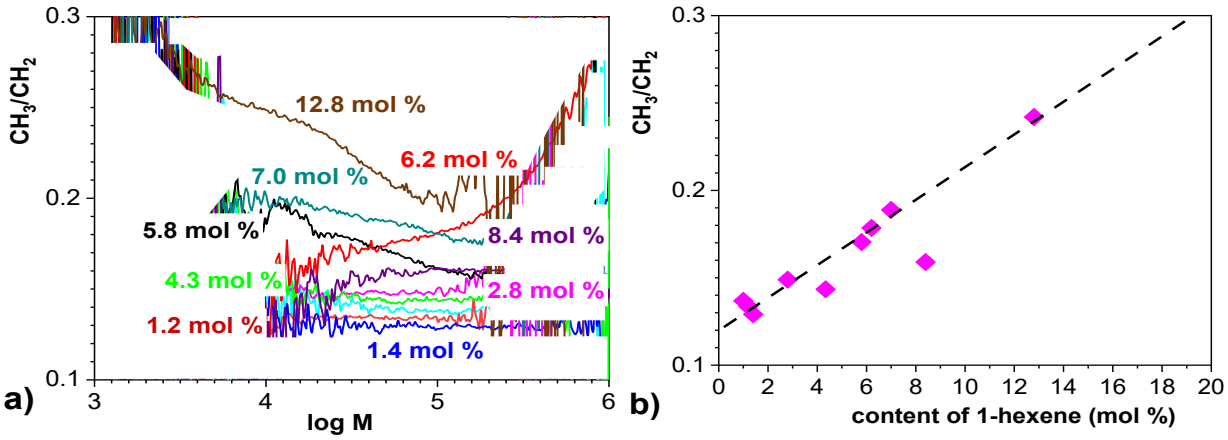

Figure 12 a) CH_3/CH_2 ratio as function of equivalent PE molar mass. b) CH_3/CH_2 ratio of the top of peaks as function of the average content of ethylene in ethylene/1-hexene copolymers (Table 4).

Repeatability, dependence on concentration and limit of detection

With the aim to check the quality of measurements with the IR5-detector, 10 solutions of an ethylene/1-butene copolymer sample were prepared and. The solutions were prepared in similar concentrations (~1.0 and ~5.0 mg/mL). Moreover, solutions with the identical concentration (1 and 5 mg/mL) were injected. The CH_3/CH_2 ratios corresponding to all measurements were calculated and the results are illustrated in Figure 13.

Figure 13 shows that reproducibility of the measurements was smaller at smaller concentration and increased with increasing concentration. We notice that noise in the data influences reproducibility of the IR5-measurements to a larger extent at smaller concentrations compared to larger concentrations. That is because the signal-to-noise ratio increases at higher concentrations.

Injections of 10 solutions with different concentrations of the ethylene/1-butene sample exhibited linear dependencies between the IR response and the polymer concentration, as illustrated in Figure 14.

Taking the base line noise of the recorded IR5-concentration signal into account, the limit of detection (defined as 3 x noise) was calculated for the tested polymer sample (Table 8). The obtained results confirm high reproducibility, linear response, and suitable detection limit of the IR5-detector. The obtained results are similar to those obtained with different polymer samples by Ortin et al. [27]. Our data confirm that changes in the CH_3/CH_2 profiles, which were described above, are many times larger than errors connected to the SEC-IR5 measurements.

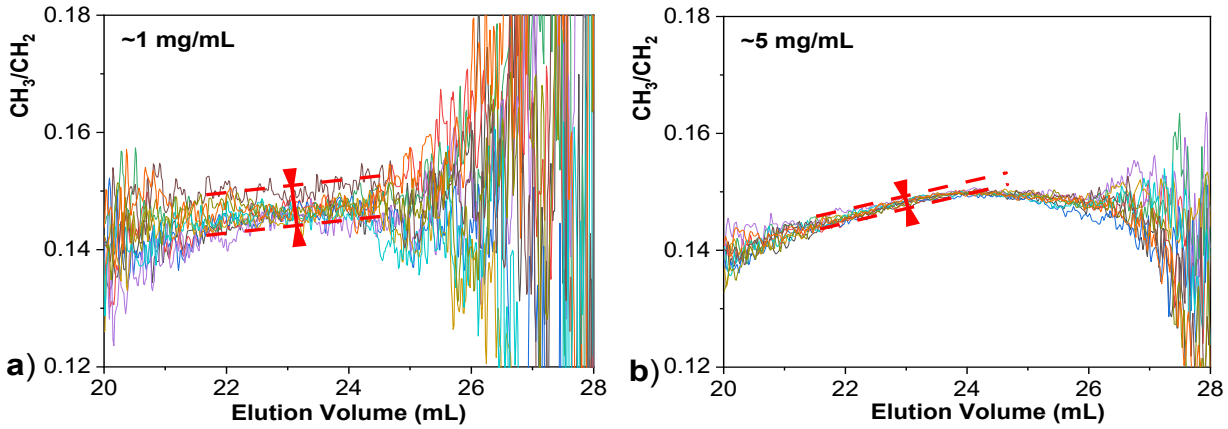

Figure 13 Ratio CH_3/CH_2 obtained after SEC-IR5 analysis of 10 solutions of ethylene/1-butene containing 5.2 wt.% of 1-butene.

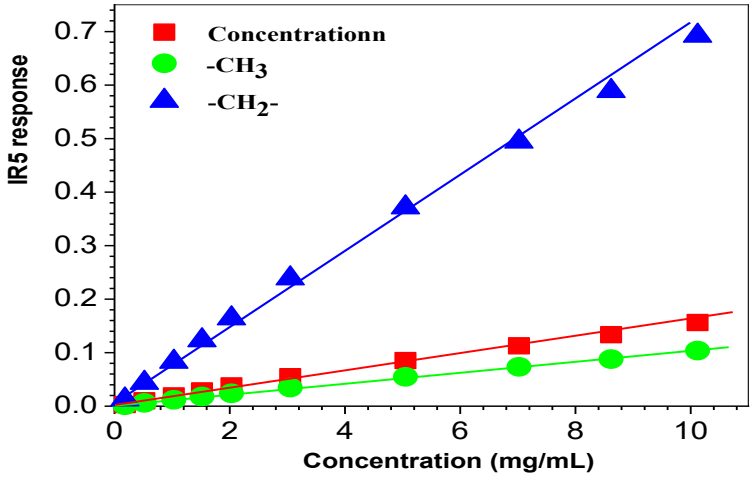

Figure 14 IR5 responses obtained after SEC-IR5 analysis of 10 solutions of EB (5.2 wt.% 1-butene) with different concentrations.

Table 8 Reproducibility and limit of detection data for the IR5.

Sample	Mean (CH_3/CH_2)	Standard deviation (CH_3/CH_2)	Limit of detection (mg/ mL)	Linearity (R^2) of concentration dependence
EB (5.2 wt. % 1-butene)	0.14483	0.000638	0.09	0.99723

Conclusion

The arms prepared at the first step were found very narrow. The star-like structures synthetized in the second step are polydisperse as the prepared macromolecules differ in the number of arms. For the first time, the star-like polymers were studied in detail by the combined SEC-MALS-Visco technique. Most of the literature equations provide values of arms per molecule far from the true ones. The only exception is Equation (6) which is approximately valid for polymers consisting of short arms. In the case of long arms, Equation (6) needs to be slightly modified by increasing the exponent 1.5 to the values of 1.6–1.7. The obtained data suggest that the longer arms require a higher exponent. However, this finding is of limited practical meaning for polymers of unknown arm length that can be only compared mutually using the average ratio $g'(M_w)$. The draining parameter of the star-like methacrylate polymers was found to be molar mass dependent within the expected range of about 0.5–1.2.

Very surprising information is that in contrast to published results for short chain branched polyethylene, the short chains in PMMA-based copolymers do not affect the intercept of the Mark-Houwink plots as described in reference [20].

For the characterization of polyolefins, it found that the high temperature SEC-IR (with a filter-based infrared detector model IR5, PolymerChar, Valencia, Spain) technique is a powerful tool for monitoring the chemical composition distribution as a function of the molar mass of various polyolefins. IR signals that correspond to methyl and methylene groups (CH_3/CH_2 ratio) along the molar mass axis of a polymer sample may be constant, increasing or decreasing with increasing molar mass. In some samples, first an increase and at lower molar masses a decrease was found. Such variations in CH_3/CH_2 profiles were found even within individual series of copolymers that were prepared with the same catalyst, including metallocene catalysts, which usually produce chemically very homogeneous polymers. It is hypothesized that one or several experimental parameters, which were eventually not strictly controlled during polymer synthesis, may cause such changes in the short chain branching distribution along the molar mass axis. Consequentially, some samples in a series exhibit different CH_3/CH_2 profiles. Monitoring the CH_3/CH_2 ratio through SEC measurements was, however, seldom performed in the past. That means the modern instrumentation can even change the generally accepted idea of molecular structure of industrial polyolefins.

References

[1] Y. Lu, L. An, Z.G. Wang, Intrinsic viscosity of polymers: General theory based on a partially permeable sphere model, Macromolecules, 46 (2013) 5731.

[2] J.R. Höhner, R.A. Gumerov, I.I. Potemkin, C. Rodriguez-Emmenegger, N.Y. Kostina, A. Mourran, J.R. Englert, D. Schröter, L. Janke, M. Möller, Globular Hydrophilic Poly (acrylate) s by an Arborescent Grafting-from Synthesis, Macromolecules, 55(2022) 2222.

[3] P.D. Gujrati, Polydisperse solution of randomly branched homopolymers, inversion symmetry and critical and theta states, The Journal of chemical physics, 108 (1998) 5089.

[4] D. Hayward, R.A. Pethrick, B. Eling, E. Colbourn, Prediction of the rheological properties of reactive polymer systems, Polymer international, 44 (1997) 248.

[5] J.H. Daly, D. Hayward, R.A. Pethrick, 2013. Prediction of the rheological properties of a curing thermoset system, Macromolecules, 46(2013) 3621.

[6] H. Stutz, K.H. Illers, J. Mertes, A generalized theory for the glass transition temperature of crosslinked and uncrosslinked polymers, Journal of Polymer Science Part B: Polymer Physics, 28 (1990) 1483.

[7] M.C. Righetti, M.L. Di Lorenzo, D. Cavallo, A.J. Müller, M. Gazzano, Structural evolution of poly (butylene succinate) crystals on heating with the formation of a dual lamellar population, as monitored by temperature-dependent WAXS/SAXS analysis, Polymer, 268 (2023) 125711.

[8] B.J. Factor, T.P. Russell, B.A. Smith, L.J. Fetters, B.J. Bauer, C.C. Han, Phase-separation kinetics of mixtures of linear and star-shaped polymers, Macromolecules, 23 (1990) 4452.

[9] O. Kalyuzhnyi, J.M. Ilnytskyi, Y. Holovatch, C. Von Ferber, Universal shape characteristics for the mesoscopic star-shaped polymer via dissipative particle dynamics simulations, Journal of Physics: Condensed Matter, 30 (2018) 215101.

[10] J. Hadar, S. Skidmore, J. Garner, H. Park, K. Park, Y. Wang, B. Qin, X.J. Jiang, D. Kozak, Method matters: Development of characterization techniques for branched and glucose-poly (lactide-co-glycolide) polymers, Journal of Controlled Release, 320 (2020) 484.

[11] B.H. Zimm, W.H. Stockmayer, The dimensions of chain molecules containing branches and rings, The Journal of Chemical Physics, 17 (1949) 1301.

[12] B.H. Zimm, R.W. Kilb, Dynamics of branched polymer molecules in dilute solution, ournal of Polymer Science, 37 (1959) 19.

[13] J. Douglas, J. Roovers, K. Freed, Characterization of branching architecture through" universal" ratios of polymer solution properties, Macromolecules, 23 (1990) 4168.

[14] J. Roovers, In Star and Hyperbranched Polymers, M.K. Mishra, S. Kobayashi, (Eds.), Marcel Dekker, New York, NY, 1999, pp. 285-341.

[15] R.W. Simms, M.F. Cunningham, High molecular weight poly (butyl methacrylate) by reverse atom transfer radical polymerization in miniemulsion initiated by a redox system, Macromolecules, 40 (2007) 860.

[16] A.M. Striegel, Specific refractive index increment (∂ n/∂ c) of polymers at 660 nm and 690 nm, Chromatographia, 80 (2017) 989.

[17] S. Podzimek, T. Vlcek, C. Johann, Characterization of branched polymers by size exclusion chromatography coupled with multiangle light scattering detector. I. Size exclusion chromatography elution behavior of branched polymers, Journal of Applied Polymer Science, 81 (2001) 1588.

[18] L. Mandelkern, In Physical Properties of Polymers, 2nd ed., J.E. Mark, (Eds.), American Chemical Society, Washington, DC, 1993, Ch. 4.

[19] I.M. Ward, Mechanical Properties of Solid Polymers, 2nd ed., J. Wiley & Sons: New York, 1983.

[20] T. Sun, P. Brant, R.R. Chance, W.W. Graessley, Effect of short chain branching on the coil dimensions of polyolefins in dilute solution, Macromolecules, 34(2001) 6812.

[21] C. Vasile [Ed.], Handbook of polyolefins, CRC press, 2000.

[22] W. Kaminsky, The discovery of metallocene catalysts and their present state of the art, Journal of Polymer Science Part A: Polymer Chemistry, 42 (2004) 3911.

[23] W. Kaminsky, G. Schupfner, Defined synthesis of copolymers using metallocene catalysis, Macromolecular Symposia, 177 (2002) 61.

[24] A.A. Alghyamah, J.B.P. Soares, Simultaneous deconvolution of the bivariate distribution of molecular weight and chemical composition of polyolefins made with Ziegler-Natta catalysts, Macromolecular rapid communications, 30 (2009) 384.

[25] Data obtained from Dr. B. Coto, University of Madrid, Spain.

[26] T. Macko, R. Brüll, R. G. Alamo, F.J. Stadler, S. Losio, Separation of short-chain branched polyolefins by high-temperature gradient adsorption liquid chromatography. Analytical and bioanalytical chemistry, 399 (2010) 1547.

[27] A. Ortín, E. Lopez, B. Monrabal, J.R. Torres-Lapasió, M.C. García-Álvarez-Coque, Filter-based infrared detectors for high temperature size exclusion chromatography analysis of polyolefins: Calibration with a small number of standards and error analysis, Journal of Chromatography A, 1257 (2012) 66.

[28] A. Ortín, J. Montesinos, E. López, P. del Hierro, B. Monrabal, J.R. Torres-Lapasió, M.C. García-Álvarez-Coque, Characterization of Chemical Composition along the Molar Mass Distribution in Polyolefin Copolymers by GPC Using a Modern Filter-B ased IR Detector, Macromolecular Symposia, 330 (2013) 63.

[29] A. Ortín, B. Monrabal, J. Montesinos, M.P. del Hierro, Application of a Multiple Linear Regression Model to Fixed Bands IR Detector Data in GPC-IR Analysis of Polyolefins, Macromolecular symposia, 282 (2009) 65.

[30] T. Frijns-Bruls, A. Ortin, J. Weusten, E. Gelade, Studies on the use of filter-based IR detector for short-chain branching characterization of polyolefin copolymers with high temperature size exclusion chromatography, Polymer, 180 (2019) 121600.

Annexes

List of Publications

H.M. Aboelanin, S. Podzimek, V. Spacek, Synthesis and molecular structure of highly compact star-like poly (methyl methacrylate) and poly (butyl methacrylate), European Polymer Journal, 194 (**2023**) 112119.

H.M. Aboelanin, S. Deshmukh, T. Macko, J.H. Arndt, S. Podzimek, R. Brüll, Monitoring the Chemical Composition of Polyolefins along the Molar Mass Axis with High-Temperature Size Exclusion Chromatography Coupled with an Infrared Detector (HT SEC-IR5), Macromolecular Symposia, 409 (**2023**) 2200174.

H.M. Aboelanin, J.H. Arndt, T. Macko, S. Podzimek, R. Brüll, Size exclusion chromatography characterization of poly (ether ether ketone), PEEK, after chemical modification, Journal of Applied Polymer Science, 140 (**2023**), e54259.

R. Pinto, G. Monastyreckis, **H.M. Aboelanin**, V. Spacek, D. Zeleniakiene, Mechanical properties of carbon fibre reinforced composites modified with star-shaped butyl methacrylate, Journal of Composite Materials, 56 (**2022**) 951.

H. Aboelanin, S. Deshmukh, T. Macko, J. Arndt, S. Podzimek, R. Brüll, Characterization of polyolefins using high-temperature size exclusion chromatography coupled with an infrared detector (HT-SEC-IR5), Peeref **2022** (poster). **https://doi.org/10.54985/peeref.2212p1310865**

Conferences

Lectures

Hamza Mahmoud Aboelanin, Stepan Podzimek, Vladimir Spacek "Synthesis, Characterization and Application of Star-like Methacrylic Polymers" 2022 *GLOBAL CONFERENCE ON POLYMERS, PLASTICS AND COMPOSITES* on March 21 - 22, **2022** at Budapest, Hungary.

Hamza Mahmoud Aboelanin, Subrajeet Deshmukh, Tibor Macko, Stepan Podzimek, Robert Brüll "Characterization of Polyolefins using High-Temperature Size Exclusion Chromatography Coupled with an Infrared Detector (HT SEC-IR5)" at *POLY-CHAR 2022 [Halle | Siegen]* Conference, May 22-25, **2022**, Germany.

Posters

Hamza Mahmoud Aboelanin, Subrajeet Deshmukh, Tibor Macko, Jan-Hendrik Arndt, Stepan Podzimek, Robert Brüll "Revealing non-reproducibility in the synthesis of LLDPE using high-temperature size exclusion chromatography coupled with an infrared detector (HT-SEC-IR5)" *8th INTERNATIONAL CONFERENCE ON POLYOLEFIN CHARACTERIZATION* (ICPC), May 21-24, **2023**, Valencia, Spain.

Hamza Mahmoud Aboelanin, Stepan Podzimek, Vladimir Spacek "Effect of Short Chain Branching on the Solution Properties of Polymethacrylates" *Seventh International Symposium Frontiers in Polymer Science*, 29 May – 1 June **2023**, The Swedish Exhibition and Congress Centre, Gothenburg, Sweden.

Participate as **Listener** at *The Forth Plastic Recyclates 2022* Conference on March 24, **2022**, at Fraunhofer Institute for Structural Durability and System Reliability LBF in Darmstadt, Germany.